Journal of Inorganic and Organometallic Polymers and Materials (2021) 31:978–996
https://doi.org/10.1007/s10904-020-01698-0

Issues in Preparation of Metal-Lignin Nanocomposites by Coprecipitation Method

Qiangu Yan[1] · **Zhiyong Cai**[2]

Received: 9 July 2020 / Accepted: 31 July 2020 / Published online: 8 August 2020

Abstract

Chemical coprecipitation technique is proven to be a beneficial method to prepare uniformly mixed catalyst metal and Kraft lignin precursors. Coprecipitation is a simple, yet very complex process which is highly sensitive to the reaction conditions, particularly temperature. In an exothermic coprecipitation process, the reaction rate can become uncontrollable over certain temperatures which could lead to a thermal runaway reaction. In this work, metal-lignin nanocomposites were synthesized by coprecipitation of metal (M) salts and Kraft lignin. Kraft lignin and metal salts were dissolved in organic solvents and DI water, respectively, to make lignin solution/suspension and metal salt aqueous solution. The aqueous solutions of metal salts were then added to the lignin solutions/suspensions and mixed well, resulting in chelation of transition metal ions to the functional groups of lignin chains and co-precipitation of metal-lignin composites from the solvents. To develop a safe process for producing M-lignin composites in a large volume, potential reactions, exothermic or endothermic processes, hazards gases, and volatiles were evaluated during the coprecipitation process. The effects of transition metal type, solvent selection, concentration of metal salts, and initial solution temperature on the interactions between metal ions and Kraft lignin, metal uniformity in the lignin matrix, and morphology of the metal-lignin composites were investigated during the coprecipitation process. Cu, Mo, Ni, and Fe were investigated as the transition metals for the metal-lignin composites. Fenton or Fenton-like reactions were discovered to occur during the Fe- and Cu-lignin coprecipitation process and tremendous heat evolved, which lead to the overshoot of the reaction system temperature in a very short time (i.e. a few seconds). Significant amounts of CO_2 and toxic NO_2 gasses were released during the coprecipitation process when Fenton or Fenton-like reactions occurred. No interaction or a very weak interaction occurred between lignin and Mo(VI) ions when mixing both solutions. Ni ions were coordinated strongly to oxygen-containing functional groups in lignin, but no Fenton or Fenton-like reaction was detected during Ni-lignin coprecipitation. Fenton reaction or Fenton-like reaction occurred when tetrahydrofuran (THF) and acetone were used to dissolve Kraft lignin, and the reaction became highly fierce and unmanageable with increasing of iron content in the composite. The reaction initialization time was shortened with increase of initial solution temperature and thermal runaway reaction might occur if the initial mixing temperature reached 60 °C or above.

Keywords Kraft lignin · Metal-lignin composites · Coprecipitation method · Fenton reaction · Process conditions · Thermal runaway

1 Introduction

Transition metals are widely used as active components for catalytic carbonization/graphitization of solid carbon sources to produce graphite, graphene, carbon nanotubes and carbon nanofibers [1]. A scalable process has been reported for massive production of few-layer graphene materials using Kraft lignin as the carbon resource [2]. One of the major issues in catalytic graphitization of solid carbon resources is the contact degree between the solid carbon sources and the metal catalyst [3]. When the metal catalyst

Electronic supplementary material The online version of this article (https://doi.org/10.1007/s10904-020-01698-0) contains supplementary material, which is available to authorized users.

✉ Zhiyong Cai
zhiyong.cai@usda.gov

[1] Ligwood LLC, Madison, WI 53705-2828, USA

[2] Forest Products Laboratory, One Gifford Pinchot Drive, USDA Forest Service, Madison, WI 53726-2398, USA

is simply mixed with lignin, a poor catalyst-lignin contact degree is obtained [3]. Lignin is a natural polymer with complex 3D structure which is chemically cross-linked to phenolic polymers with huge molecules. In efficient catalytic graphitization of lignin, the uniformly mixed catalyst metal and lignin precursors must be prepared before the conversion process. The uniform metal-lignin mixture is a kind of metal-polymer nanocomposite in which metal species are well fixed or anchored in the polymer matrices [4]. To get high performance metal-polymer nanocomposites, metal nanoparticles must be well dispersed in polymer matrices. Many physical–chemical techniques have been developed and utilized to produce metal-polymer nanocomposites: evaporation and sputtering methods [5, 6]; plasma deposition [7]; UV-radiation curing [8]; deposition via cluster sources [9]; laser ablation [10]; electro-polymerization [11]; surface functionalization [12]; and ion implantation [13]. However, most of these techniques are limited to prepared metal-polymer thin films and membranes [14]. To prepare the bulk metal-polymer composite samples, some wet chemical techniques are often used. These methods include in situ and ex situ approaches [15]. In the ex situ method, nanoparticles (NPs) are first prepared through chemical methods by which particle size and shape of NPs can be controlled [16]. NPs are then dispersed in a polymer or a monomer solution for successive polymerization. NPs are likely to agglomerate which leads to weak interaction between metal and polymer, therefore, these metal nanoparticles are usually functionalized with organic tails to increase their solubility and stability in a solution [17]. To simplify the production process and reduce cost, NPs are frequently produced in situ within the polymer by chemical reduction of a metal salt or the decomposition of a metal complex [18].

Lignin is a natural polymer; we cannot utilize ex-situ methods to synthesize metal-lignin nanocomposites. As a huge, complex 3-D polymer, it is very difficult for metal particles to uniformly distribute into lignin molecules using direct mixing methods, and very poor graphitization degree was obtained for the mixture of metal nanoparticles and lignin samples [3, 4]. Metal salts are used to synthesize metal-lignin composites [19]. Metal salts, in contrast to metal powder, are assumed to be easily distributed into lignin, since there are significant amounts of O-, S- and/or N-based functional groups in lignin structures. The strategy to uniformly disperse metal ions into huge 3D lignin molecules is to chelate metal ions to functional groups and form M–O, M-S, or M–N bonds when mixing lignin and metal salts in an appropriate way [3, 20]. In many cases, metal-biomass mixtures are often made by incipient wetness method [21], where metal-salt solution is added to a dry biomass material and the metal salt solution is absorbed into the inner pores of the biomass through capillary action. Metal ions drawn into the biomass will further diffuse into the biomass matrix and are anchored to oxygen-containing functional groups [22]. Due to its production process, Kraft lignin is highly hydrophobic and, generally, impermeable to water, therefore metal salt aqueous solutions will be repelled from the Kraft lignin surface. A low metal dispersion was observed in metal-Kraft lignin mixtures obtained through an aqueous impregnation method [3, 4]. Therefore, a proper method should be employed to ensure the initial homogeneous distribution of metal salts into the lignin to achieve high metal dispersion in metal-lignin composites.

To uniformly distribute metal ions in lignin, metal-lignin composites are prepared using a 'coprecipitation' technique [3], where Kraft lignin and metal salts are each dissolved in a selected solvent. An aqueous solution usually is prepared by dissolving metal salt in de-ionized (DI) water; Kraft lignin is often dissolved or dispersed in a proper organic solvent. Metal salt and lignin will coprecipitate as solid particles after mixing both solutions. Metal ions will diffuse into the inner surface of Kraft lignin, then chelate and react with functional groups of lignin chains during the mixing and precipitation process. The M-lignin nanocomposites are obtained after vaporizing the solvents. Coprecipitation is one of the most widely used techniques for preparing nanoparticles, nanocomposites, and catalysts [23]. Coprecipitation synthetic method [24] is one of the simplest approaches for synthesizing nanostructured metal particles, oxide nanoparticles, and metal chalconides. This method presents some advantages [25]: it is simple and economical, has a practical preparation process, yields a uniform component distribution, involves relatively low reaction temperature, particle size and composition is controllable, and usually no organic solvent is involved. However, there are several limitations of the coprecipitation method: chemical precipitation is kinetically not a controlled process, and the coprecipitation process is highly sensitive to the reaction conditions. Therefore, the particle size distribution, particle morphology, and the reaction degree of the synthesized solids are affected by the precipitation process conditions such as type of metal, metal precursor compounds, metal oxidation states, concentration of metal salts, mixing temperature, pH values of the solutions, solvents used, and evaporation conditions. These variables affect the nanoparticle growth, aggregation, and deposition from the solvent.

To scale-up the lignin-to-graphene process, massive production of M-lignin composites is needed. While chemical precipitation is a simple procedure, it is a complex process and the reaction rate is sometimes uncontrollable for an exothermic coprecipitation process which could lead to a thermal runaway reaction. To date, limited research has been done on this topic. The purpose of this study is to develop a reliable process for mass production of uniformly dispersed metal-lignin composites. Metal-lignin composites are to be prepared by coprecipitation method in conjunction with

exploration of new conditions applied to a safe chemical coprecipitation process. Some critical issues will be evaluated to develop a safe process for the production of M-lignin composites in a large volume: (i) potential reactions (including possible undesired reactions) as well as an exothermic or endothermic coprecipitation process should be first identified and managed to produce M-lignin composites accordingly; (ii) non-condensable gases and volatiles evolved from the chemical coprecipitation process; and (iii) understanding the effects of process conditions on the product properties, process phenomena, and safety issues during the coprecipitation stage. The important factors include effects of different transition metal ions, solvents used for dissolution of kraft lignin, metal/lignin mass ratio, and the initial temperature of the coprecipitation process. The results of these investigations will then be used in the developed graphene growth model from kraft lignin and help determine the critical process variables for the scalable production process.

2 Materials and Method

2.1 Chemicals and Materials

Three solvents and water were used in this experiment. The solvents methanol (≥ 99.9%), acetone (≥ 99.9%), and tetrahydrofuran (THF, anhydrous, ≥ 99.9%, inhibitor-free) were all purchased from Sigma-Aldrich, Inc. (St. Louis, MO, USA). Copper nitrate tetrahydrate ($Cu(NO_3)_2{\cdot}4H_2O$), nickel nitrate hexahydrate ($Ni(NO_3)_2{\cdot}6H_2O$), ammonium molybdate tetrahydrate ($(NH_4)_6Mo_7O_{24}{\cdot}4H_2O$), iron(III) nitrate nonahydrate ($Fe(NO_3)_3{\cdot}9H_2O$ were also obtained from Sigma-Aldrich. Kraft lignin (BioChoice, Plymouth, NC, USA) was supplied by Domtar Corp. ASTM D4442-07 standard was used to test the proximate moisture in Kraft lignin [26]. The ash content in Kraft lignin was 1.65 wt% measured following ASTM D1102 standard [27]. The average molecular weight and molecular weight distribution of Kraft lignin were measured using gel permeation chromatography (GPC); the results showed Mn = 988 ± 56 g/mol, Mw = 6672 ± 315 g/mol. Lignin elemental analysis was analyzed on an elemental analyzer. The mineral analysis was performed using an ICP Optical Emission Spectrometry system (Agilent 5800 ICP-OES Spectrometer, Santa Clara, CA, USA). The elemental compositions are summarized in Tables 1 and 2.

Table 1 Weight percentages (wt%) of C, H, O, N, and S in Kraft lignin (ash free)

Elements	C	H	O	N	S
Raw lignin	64.7 ± 0.5	6.4 ± 0.4	27.9 ± 1.0	0.1 ± 0.03	0.9 ± 0.1

2.2 Metal-Lignin Composites Preparation

Metal-lignin composites in current work were prepared by chemical coprecipitation method as illustrated in Scheme 1.

2.2.1 Metal-lignin Composites with Different Transition Metals

The metal-lignin composites with different transition metals were prepared by the coprecipitation method in a chemical fume hood as follows. For the copper-lignin composite, 100 g of Kraft lignin was dissolved in 150 mL tetrahydrofuran and stirred at 45 °C for 60 min; a thermocouple was fixed in the solution to monitor the temperature. 42.7 g of copper nitrate tetrahydrate was dissolved in 50 mL DI water and stirred at 45 °C for 30 min. Following that, copper nitrate solution was poured into Kraft lignin solution and stirred robustly; the temperature of the solution was recorded during the mixing process. To monitor the potential reactions occurring during the blending process, a Hiden QGA quantitative gas analysis system was used to measure the volatile species released from the reaction system. The signals from the mass spectra of 18, 31, 44, 47, 58 and 72 (m/z) were identified as the evolved gases from the chemical coprecipitation process as well as volatile solvents and were identified as H_2O, CH_3OH, CO_2, NO_2, acetone and tetrahydrofuran, respectively. The mixture was dried at room temperature in the hood to vaporize the solvents naturally for one week, and the dried sample was denoted as Cu-lignin.

For the nickel-lignin composite, Kraft lignin solution (100 g Kraft lignin in 150 mL tetrahydrofuran) was prepared and stirred at 45 °C for 60 min. Nickel nitrate solution (56.2 g nickel nitrate hexahydrate in 50 mL DI water) was mixed and stirred at 45 °C for 30 min. Following that, both solutions were blended and stirred vigorously. The temperature and the volatiles from the mixture were also monitored and recorded. The mixture was dried at room temperature for one week, and the sample was labeled as Ni-lignin.

For the preparation of molybdenum-lignin composite, 46.4 g of ammonium molybdate tetrahydrate was dissolved in 50 mL DI water and stirred at 45 °C for 30 min. Then

Table 2 Mineral elements Kraft lignin sample

Mineral elements	P	K	Ca	Mg	Fe	Mn	Zn	Cu	B
	%				Ppm				
Kraft lignin	0.02	0.06	0.03	0.02	25	23	12	2	21

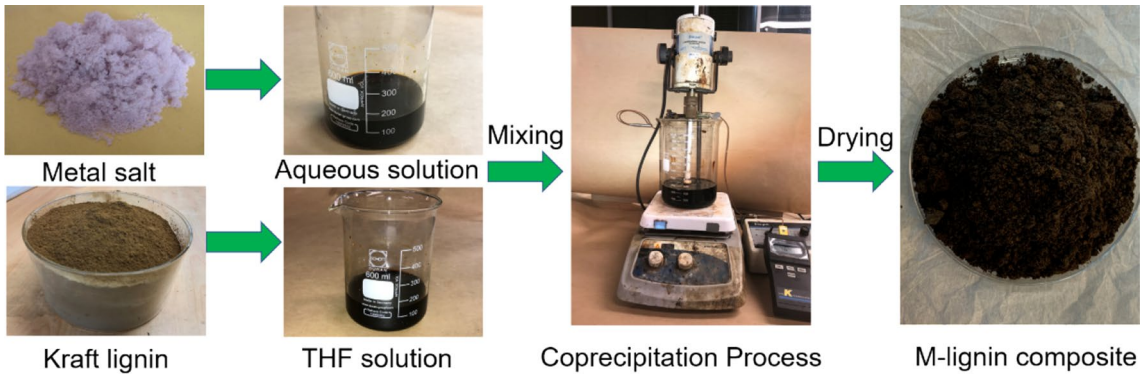

Scheme 1 Preparation of M-lignin composites by chemical coprecipitation method

ammonium molybdate solution was added to Kraft lignin solution (100 g Kraft lignin in 150 mL tetrahydrofuran) and stirred strongly. The mixture was dried at room temperature for one week, and the sample was identified as Mo-lignin.

For the iron-lignin composite, 82 g of iron (III) nitrate nonahydrate was dissolved in 50 mL DI water and stirred at 45 °C for 30 min. The iron nitrate solution was then added to Kraft lignin solution (100 g Kraft lignin in 150 mL tetrahydrofuran) and stirred energetically. The mixture was dried in the hood at room temperature for one week, and the sample was described as Fe-lignin.

2.2.2 Preparation of Fe-lignin Nanocomposites with Different Solvents

Fe-lignin composites were prepared at 50 °C using a co-precipitation technique. Kraft lignin was dissolved or dispersed in different solvents to form solutions or suspensions [3]: 100 g of Kraft lignin was mixed with each of four different solvents (150 mL each), i.e., de-ionized (DI) water, methanol, acetone, and THF respectively, and the Kraft lignin solutions or suspensions were stirred at 50 °C for 60 min. The aqueous iron nitrate solution was prepared by adding 82 g of iron (III) nitrate nonahydrate to 50 mL DI water, then stirred at 50 °C for 30 min. The iron nitrate solution was poured into lignin solutions or suspensions, respectively. The mixture of iron nitrate and lignin solutions was stirred robustly. The temperature and the volatiles from the mixtures were also monitored and recorded. The obtained iron-lignin mixtures were put in the hood at room temperature for one week. The Fe-lignin composites prepared using 4 different solvents are labeled as Fe-lignin-W (water), Fe-lignin-M (methanol), Fe-lignin-A (acetone), and Fe-lignin-T (THF).

2.2.3 Preparation of Fe-lignin Composites with Different iron-lignin Ratios

Four iron nitrate solutions were prepared by adding different amounts of iron nitrate nonahydrate (38.9 g, 82.0 g, 130.4 g, and 187.7 g) to four different volume levels of DI water (25 mL, 50 mL, 75 mL, and 100 mL) [4], respectively, and all four solutions were stirred at 45 °C for 30 min. Each of these four iron nitrate solutions was added to its respective Kraft lignin solution (100 g lignin in 150 mL tetrahydrofuran at 45 °C). The prepared Fe-lignin composites were kept at room temperature in the hood for one week, and the samples were named as 5%-Fe-lignin, 10%-Fe-lignin, 15%-Fe-lignin, and 20%-Fe-lignin.

2.3 Analysis and Characterization

The ATR-FTIR spectra of Kraft lignin, and M-lignin composites were recorded with the Thermo Scientific ATR-FTIR spectrometer (Thermo Scientific, Nicolet iZ10) at a resolution of 4 cm^{-1} for 64 scans in 500 to 4000 cm^{-1} range. FTIR spectra were used to determine structural changes of Kraft lignin in M-lignin composites. The morphology of M-lignin composites was examined using a Field Emission Scanning Electron Microscope (FESEM, JEOL JSM-6500F) equipped with energy dispersive X-ray spectroscopy (EDS) analyzer allowing for surface elemental mapping of samples. All SEM samples were pre-coated with 10 nm Pt and the FESEM system was operated with an accelerating voltage of 10 kV [3].

3 Results and Discussion

Metal-lignin composites were synthesized by coprecipitation technology, where transition metal species were in-situ formed and dispersed into lignin matrices through a chemical coprecipitation process. Inorganic salts used as metal precursors are first dissolved in DI water to obtain homogenous solutions of metal ions, while Kraft lignin solutions or suspensions were obtained after dissolving or dispersing Kraft lignin in different organic solvents. After adding iron nitrate solution to Kraft lignin solution/suspension, solid Fe-lignin particles deposited from the solvents. A uniformly dispersed M-lignin composite could be achieved through this in-situ approach where metal ions are attached by coordinate bonds to O-, S-, and N- containing functional groups in lignin during the blending and precipitating process. Metal-lignin combinations start precipitating when the critical concentration of species is attained followed by nucleation and growth phases [28]. The structure, uniformity, morphology, metal oxidation states, and size and shape of metal species particles of the metal-lignin composites are greatly influenced by type of transition metal, solvent used in the solution, initial solution pH value, temperature, and concentration of metal salt [29].

3.1 Four M-lignin Composites with Different Transition Metals

Transition metals have been tested for catalytic graphitization of solid biomass resources to graphene-based nanomaterials [30]. The transition metal ions selected for the present work are Fe(III), Ni(II), Cu(II), and Mo(VI, $(Mo_7O_{24})^{6-}$) to prepare metal-lignin nanocomposites as the precursors for production of graphene materials. The metal-lignin composites with different transition metals were prepared by the coprecipitation method. After mixing the metal salt aqueous solution and the lignin THF solution, the coprecipitation reactions behaved distinctively different for each metal based on process temperature, gaseous products, and physical appearances of the solid products.

The solution temperature (Ts) of metal-lignin was measured by a thermocouple fixed at the center of the mixture. Sample temperature vs reaction time is plotted in Fig. 1. Temperature of the mixture changes after adding the metal aqueous solution to the lignin solution due to the heat liberated during the coprecipitation process. The temperature profiles in Fig. 1 indicate the differences in heat generation during the coprecipitation process of the different metal-lignin composites. Heat generation during the

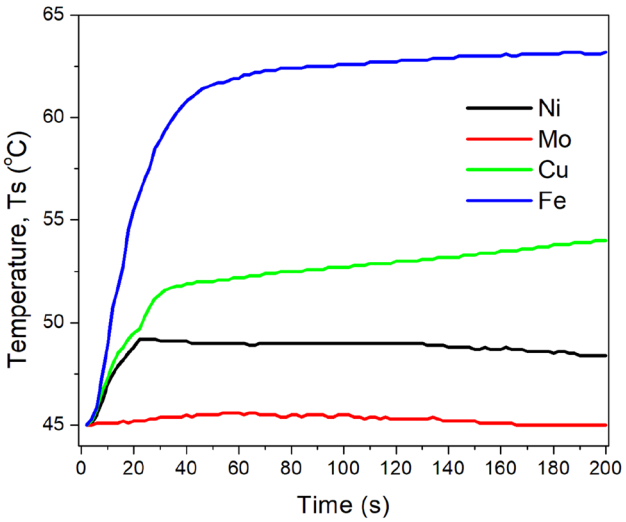

Fig. 1 Temperature profiles during preparation of metal-lignin composites with different transition metals (reaction conditions: start temperature, 45 °C; metal content, 10 wt%; salt solvent, DI water; lignin solvent, tetrahydrofuran)

metal-lignin coprecipitation process can be from several sources. First, the enthalpy of mixing (or heat of mixing) is the heat released or absorbed from the mixing of both the metal salt solution and the lignin solution [31]. During the mixing process, metal ions may diffuse, or transfer to the lignin molecule surface, and form a coordinated bond to heteroatom (O, S, and N) -containing functional groups in Kraft lignin, where metal-lignin complexes are formed. The heat of mixing is the consequence of the formation of new bonds between metal ions and the functional groups of lignin; the enthalpy of mixing can be exothermic or endothermic. Second, the temperature change may result from the heat of precipitation which is the energy change when a precipitate is formed from its original ions in the solution. The precipitation process can be an exothermic or endothermic reaction. Third, reaction heat comes from chemical reduction of metal ions by active functional groups in lignin or Fenton-like reactions catalyzed by transition metal ions. Chemically, lignins are cross-linked phenolic polymers and phenolic units are the basic structures of lignins. Much work has been done on degradation of lignin through Fenton or Fenton-like reactions [32]. A Fenton reaction is a rapid and exothermic process where organic compounds are oxidized to carbon dioxide and water by Fenton reagents [33].

During the Mo-lignin composite preparation process, Ts of Mo-lignin mixture was kept nearly constant at 45 °C. From the beginning, it increased to 45.6 °C after adding ammonium molybdate solution to the lignin solution, then decreased slowly to 45.0 °C after mixing for 200 s. To monitor the potential reactions which occurred during the

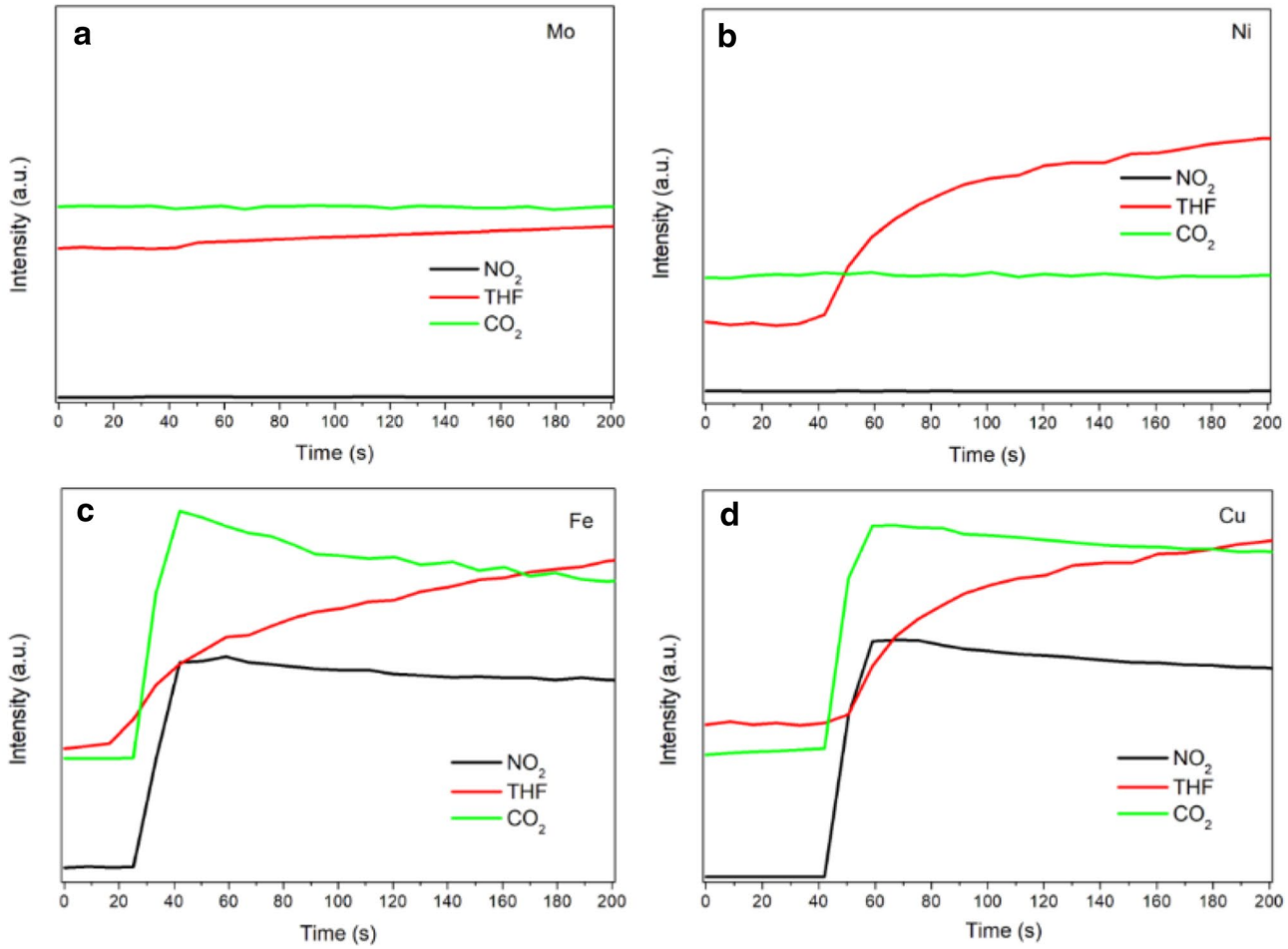

Fig. 2 CO_2, NO_2 and THF concentration levels by an on-line mass spectrometer during preparation of metal-lignin composites with different transition metals (reaction conditions: start temperature, 45 °C; metal content, 10 wt%; salt solvent, DI water; lignin solvent, tetrahydrofuran)

blending process, a residual gas analysis (RGA) was used to measure the volatile species released from the reaction system (Fig. 2). No gaseous or volatile products formed during Mo-lignin co-precipitation process (Fig. 2a). A thick slurry mixture was formed during the stirring process and no immediate solid deposited from the mixed solutions.

For the Ni-lignin composite, Ts of Ni-lignin mixture increased immediately from 45 °C to 49.2 °C after mixing nickel nitrate solution and lignin solution for 22 s, then decreased gradually to 48.4 °C after mixing for 200 s. Figure 2b shows only THF concentration level increased due to the vaporizing under increased temperature during the coprecipitation process. A sticky syrup-like product was formed during the mixing process.

For the Fe-lignin composite, Ts of Fe-lignin mixture increased rapidly from 45 °C to 60.8 °C after mixing iron nitrate solution and lignin solution for 40 s, then increased gradually to 63.2 °C after mixing for 200 s. Figure 2c plots the trends of gas species during coprecipitation of the Fe-lignin sample. A significant amount of CO_2 and NO_2 started to release after mixing for 25 s. CO_2 concentration level increased fast and reached its maximum level after reaction for 54 s, then decreased slowly to low levels. NO_2 formation rate increased to its high level after reaction for 59 s, then kept near constant. CO_2 and NO_2 are the most probable products during catalytic oxidation of lignin by Fenton reaction.

Similar to the Fe-lignin composite, Ts of Cu-lignin mixture increased quickly from 45 °C to 51.6 °C after mixing copper nitrate solution and lignin solution for 32 s, then increased gradually to 54.0 °C after mixing for 200 s. CO_2 and NO_2 were also observed to be released from Cu-lignin mixing system during the precipitation process; it seemed they were the products of catalytic oxidation of lignin by a Fenton-like reaction.

Lignin possesses abundant hydroxyl, carboxyl, carbonyl, phenolic, ether, and lactone groups which can serve as ligands to catch metal ions by coordinate bonding. When mixing lignin with transition metal solutions, metal ions may be chelated by these functional groups and form metal-lignin

complexes. However, due to the different metal properties like oxidation states, electron structures of their ions, etc., these four metals show significantly distinct interaction behaviors with lignin during coprecipitation process.

Because Mo(VI) presents as an oxo-anion such as $(MoO_4)^{-2}$, or $(Mo_2O_7)^{-2}$, and $(Mo_7O_{24})^{6-}$ in ammonium heptamolybdate solution, it is highly unlikely to chemically adsorb onto the lignin surface where negatively charged oxygen-containing functional groups prevail. Instead, ammonium cations (NH_4^+) might combine with these oxygen-containing ligands. No interaction or a very weak interaction occurs between lignin and Mo(VI) ions when mixing both solutions, which may explain why the temperature kept constant and no gaseous products were detected during the precipitation process. A thick slurry mixture was formed after stirring the mixture for 30 min. A brown powder product was obtained as the Mo-lignin composite sample after vaporizing the solvent at room temperature for one week (Fig. 3); its physical appearance was more like Kraft lignin except a little darker in color.

Ni ions (Ni^{2+}) may be coordinated strongly to oxygen-containing ligands in lignin, while significant heat was liberated during the chelating process. Consequently, combined Ni ions in lignin will significantly modify the molecular structure of lignin by drawing the coordination sites in closer, thereby making the lignin structure tighter and more condensed [4]. This is a very quick process, and considerable solvents, including THF and water, were trapped in the Ni-lignin composite when the lignin structure began to shrink and condense during the coprecipitation process. This leads to a syrup-like product being formed during the mixing process. The Ni-lignin composite sample looked like a dark grey homogeneous lump since there were still some solvents trapped in the mixture after drying at room temperature for one week (Fig. 3). No redox reactions happened during Ni-lignin composite formation process since no CO_2 or other gaseous products were detected (Fig. 2b).

Fig. 3 Physical appearance of Kraft lignin, and Mo-lignin, Ni-lignin, Cu-lignin, and Fe-lignin composites. (Reaction conditions: start temperature, 45 °C; metal content, 10 wt%; salt solvent, DI water; lignin solvent, tetrahydrofuran)

When mixing with lignin solution, Fe^{3+} ions are chelated to hydroxyl, carboxyl, carbonyl, phenolic, ether, and lactone groups in lignin and a uniform solution is first obtained. The temperature began to rise after blending for 5 s and as the temperature reached 58.0 °C (after mixing for 25 s) (Fig. 1), the mixture became thicker with brown gases and vapor bubbling out from the sticky mixture. With the reaction ongoing, the temperature increased continuously with more gases and vapor generated in the mixture and the volume of the mixture expanded approximately 3–5 times as a foam state. The foam collapsed after all the solvents evaporated and a dark grey powder product was achieved (Fig. 3). Heat and gaseous products during Fe-lignin coprecipitation were mainly contributed by the Fenton reaction or Fenton-like reaction [34]. The chelated Fe^{3+} could be reduced to Fe^{2+} by active functional groups [35] (Eq. 1).

$$Fe^{3+} + CxHyOz \rightarrow Fe^{2+} + H^+ + H_2O + CO_2 \quad (1)$$

Tetrahydrofuran was used as the solvent to dissolve Kraft lignin where a trace of tetrahydrofuran peroxide may form when contacting air. THF peroxide then reacts with water to generate H_2O_2 (Eq. 2) when mixing with water solution.

$$ROOH + H_2O \rightarrow ROH + H_2O_2 \quad (2)$$

Generally, Fe^{2+} can react with peroxides such as H_2O_2 to produce hydroxyl radicals (OH·) (Eq. 3), which is well-known as the Fenton reaction [36]. Fe^{3+} can also react with H_2O_2 in the so-called Fenton-like reaction (Eq. 4) [37]. OH· can also be initially generated by interaction of Fe^{2+} and Cu^+ with oxygen (O_2) [38].

$$Fe^{2+} + H_2O_2 \rightarrow Fe^{3+} + HO\cdot + OH^- \quad (3)$$

$$Fe^{3+} + H_2O_2 \rightarrow Fe^{2+} + HOO\cdot + H^+ \quad (4)$$

Hydroxyl radicals will initialize the oxidation of organic compounds through radical reactions (Eqs. 5–6) [39], where H_2O and CO_2 are the main products. Usually, Fenton reaction takes place at room temperature and under atmospheric pressure and reaction rates are relatively

fast since it's a radical reaction. The reaction is strongly affected by the pH value and the process is promoted under acidic environment. The initial pH value of the Fe-lignin mixture is in the range of 3–4. Nitric acid may be formed and subsequently oxidize active functional groups in lignin to CO_2 and H_2O, while at the same time, nitrogen oxides are released (Eq. 8).

$$HO\cdot + RH \rightarrow R\cdot + H_2O \quad (5)$$

$$HO\cdot + R-COOH \rightarrow R\cdot + H_2O + CO_2 \quad (6)$$

$$H^+ + NO_3^- \rightarrow HNO_3 \quad (7)$$

$$HNO_3 + CxHyOz \rightarrow H_2O + CO_2 + NO_2 \quad (8)$$

Aside from Fe^{2+}/ Fe^{3+} ions serving as the catalysts for the Fenton reaction, the process promoted by cations such as Cu^{2+}, Co^{2+}, and Mn^{2+} is called a ''Fenton-like reaction'' [40]. Cu^{2+} has been widely studied for Fenton-like reactions in pollution remediation [41], solar energy [42], and sensors [43]. Like the Fe-lignin sample, a Fenton-like reaction was also found to take place in the Cu-lignin precipitation process. A large amount of NO_2 and CO_2 gas as well as solvent vapors were observed to be released from the mixture. A dark grey powder product is attained (Fig. 3).

The FTIR spectra of Kraft lignin and Metal-lignin composites are plotted in Fig. 4. The representative FTIR peaks were assigned to functional groups in lignin [44]. A strong FTIR peak at 3368 cm^{-1} is assigned to stretching vibrations of hydroxyl groups in lignin. Peaks at 2937 and 2841 cm^{-1} are assigned to stretching vibrations of methyl and methylene groups in branch chains [45]. FTIR bands at 1710 cm^{-1} is contributed by carbonyl groups. Absorption peaks at around 1597, 1511, and 1417 cm^{-1} are associated with vibrations of aromatic units in lignin [46]. The peaks at 1265 and 1215 cm^{-1} are contributed by the C=O stretch and C–C, C-O, and C=O stretches, respectively [47, 48]. The peak at 1078 cm^{-1} is assigned to C-O deformation in secondary alcohol and aliphatic ether in side-chains [35].

FTIR spectrum of Mo-lignin composite is compared in Fig. 4. There were several new peaks for the Mo-lignin sample. The N–H stretching vibration of NH_4^+ was detected at 3170 cm^{-1} and the N–H deformation band of ammonium ions appeared at 1417 cm^{-1} [49]. The three bands (926, 877 and 835 cm^{-1}) below 1000 cm^{-1} were contributed by various Mo–O lattice stretching modes of polymolybdates [50]. No change was found for all the peaks related to Kraft lignin which proved no interaction or a very weak interaction occurred between lignin and Mo(VI) ions in the Mo-lignin sample.

FTIR spectra of the Ni-, Cu-, and Fe-lignin composites were compared to Kraft lignin in Fig. 4. Intensity and position of FTIR bands were found to be reduced and/or shifted after introducing nickel, copper and iron ions. First, the peaks of hydroxyl groups (3700–3300 cm^{-1} and 1100–900 cm^{-1}) were decreased in intensity or shifted in positions, indicating a decline of free hydroxyl groups on the Kraft lignin. The new band observed at 3240 cm^{-1} is assigned to metal hydroxides formed in M-lignin (M = Ni, Cu, and Fe) [51]. The decrease in intensity and shift of peaks related to –C=O, C–O–C and –COO groups (1710, 1665, 1456, 1362, 1210, and 1078 cm^{-1}) means strong interaction between nickel, copper, and iron ions

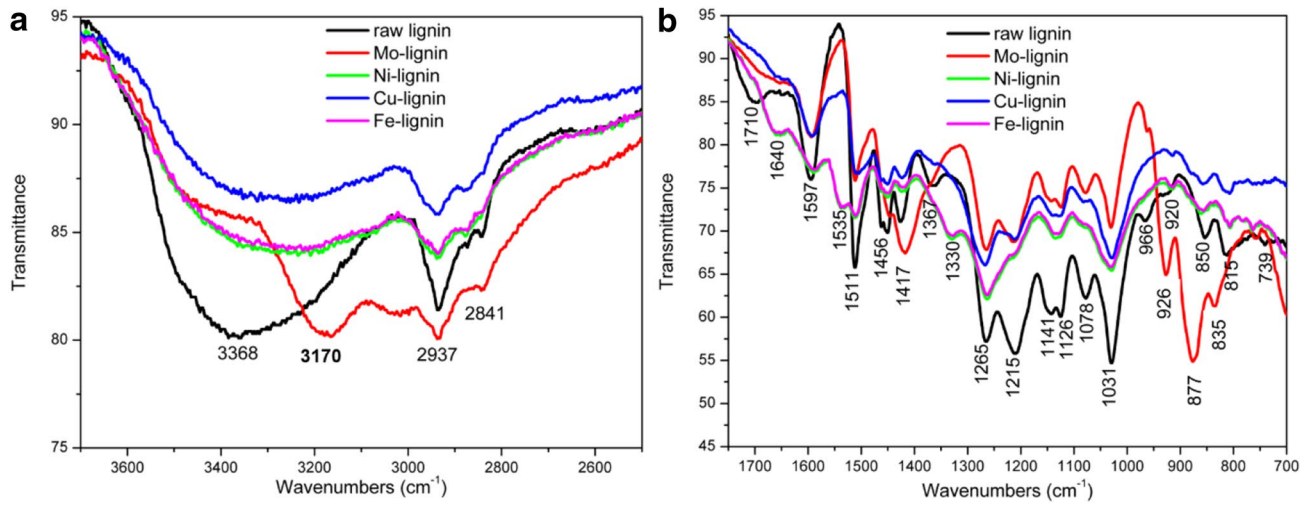

Fig. 4 FTIR spectra of Kraft lignin, and Mo-lignin, Ni-lignin, Cu-lignin, and Fe-lignin composites at the ranges of 3700 to 2500 cm^{-1} (**a**) and 1750 to 700 cm^{-1} (**b**)

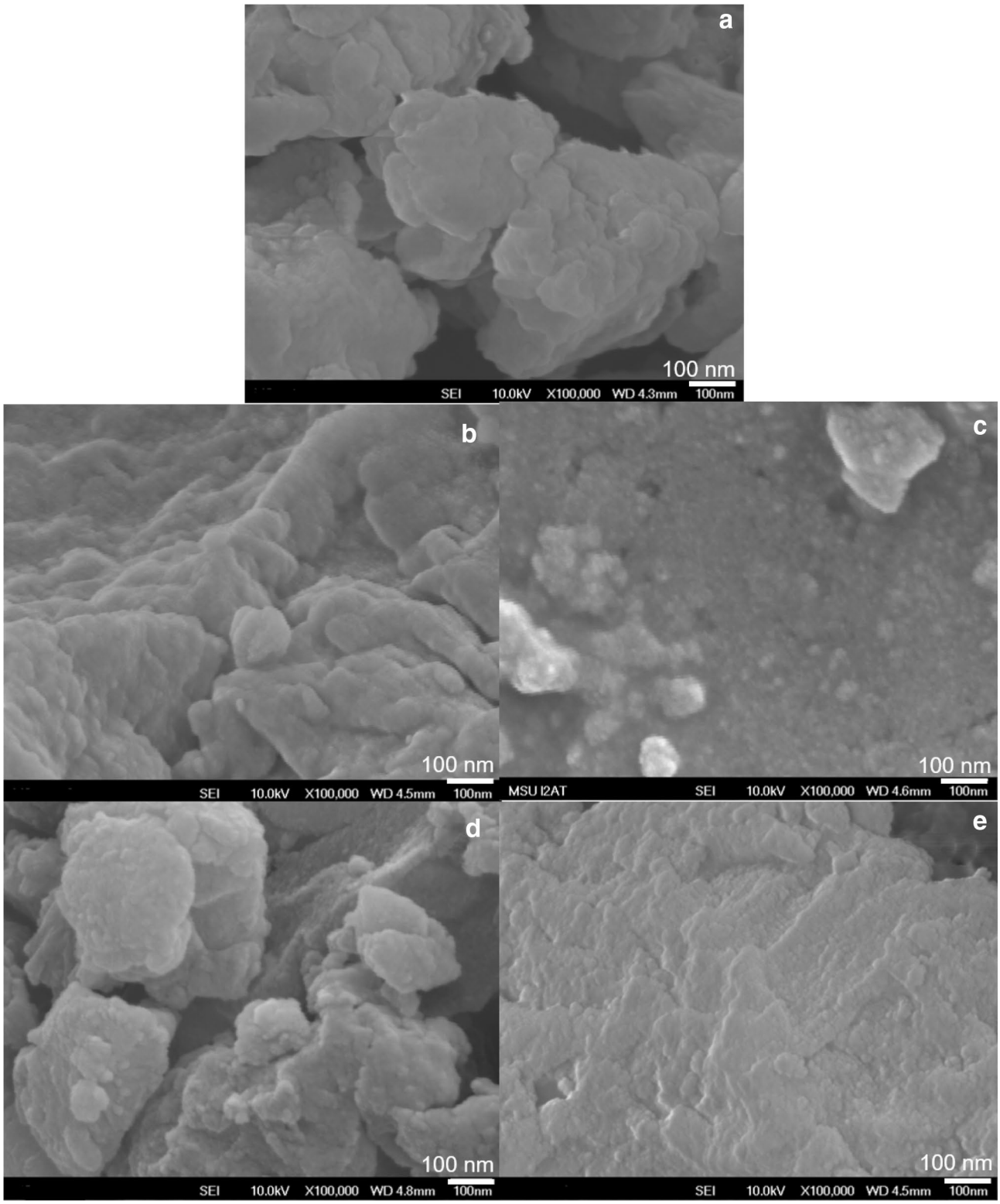

Fig. 5 SEM images of Kraft lignin (**a**), Cu-lignin (**b**), Ni-lignin (**c**), Mo-lignin (**d**), and Fe-lignin (**e**) composites

and the these functional groups [35]. FTIR spectra changes in $-OH$, $-C=O$, $C-O-C$ and –COO might be related to the coordinated bonds formed between metal ions and carboxylate and hydroxylate anions since carbonyl, carboxyl, and hydroxyl groups are the main ligands to combine nickel, copper, and iron ions [35, 52]. Aromatic ring structures in

M-lignin composites were not modified since no obvious changes were detected in FTIR bands of aromatic units (1594, 1511, 1426, 1265, 1124, and 1031 cm^{-1}) The new FTIR bands at 1535 and 1330 cm^{-1} were assigned to surface nitrate complexes from metal nitrates [53–55].

FESEM was used to analyze the morphology of Kraft lignin and M-lignin samples. Figure 5 shows the morphologies of the Kraft lignin and the M-lignin composites. The particle size of Kraft lignin is between 0.5–1 µm and its surfaces are smooth and clean (Fig. 5a). Figure 5b shows a SEM image of Cu-lignin sample; the sample looks porous and embedded with nanoparticles. The dried Ni-lignin sample is made of pores filled with 10–50 nm particles (Fig. 5c). Figure 5d shows a SEM image of Mo-Kraft lignin samples; the morphology of Mo-lignin is similar to that of Kraft lignin, but its surface is embellished with some particles. Figure 5e shows a SEM image of Fe-Kraft lignin samples; the Fe-lignin composite is embedded with porous nanoparticles. These nanoparticles have sizes ranging from 2–8 nm. SEM results agree with HRTEM results reported in our previous work [30]. Figure S1 shows the elemental mapping of C, Fe and O for a 10% Fe-lignin composite. It was observed that iron ions were uniformly anchored in the kraft lignin matrix.

3.2 Fe-lignin Composites Prepared with Different Solvents

Chemical coprecipitation method is used to prepare uniformly distributed metal-lignin composites [3]. Metal salts are dissolved in water to form aqueous metal ion solutions, therefore the ideal solvents to dissolve or disperse Kraft lignin should be miscible with water [3]. In present work, DI water, methanol, acetone and tetrahydrofuran are chosen to dissolve/disperse Kraft lignin. Four, 10 wt% Fe-lignin composites were prepared using these four different solvents (DI water, methanol, acetone, and THF) by coprecipitation methods, and the Fe-lignin composites from 4 different solvents are Fe-lignin-W, Fe-lignin-M, Fe-lignin-A, and Fe-lignin-T [3]. Kraft lignin demonstrates different solubility in DI water, methanol, acetone and tetrahydrofuran. A light brown suspension was obtained when mixing kraft lignin and water together at room temperature and nearly all the Kraft lignin precipitated from the water after settling for 30 min, indicating Kraft lignin is totally insoluble in water at low temperature. Dark brown solutions were initially achieved after mixing Kraft lignin with methanol, acetone, and THF; however, after standing for 30 min, approximately 35% of lignin deposited from methanol and 20% of lignin deposited from acetone. No Kraft lignin settled from THF solution after standing for 30 min. The chemical coprecipitation processes for Fe-lignin-W, Fe-lignin-M, Fe-lignin-A, and Fe-lignin-T composites demonstrate distinct reaction phenomena, i.e., different temperature profiles, gas formation, and physical

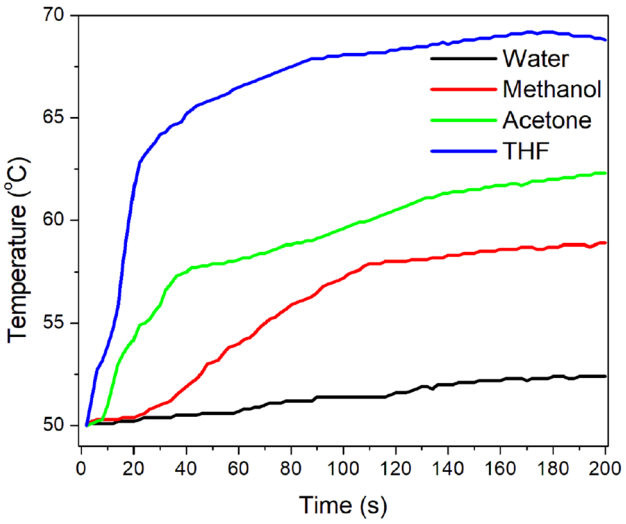

Fig. 6 Temperature profiles during preparation of 10 wt% Fe-lignin composites with different solvents (reaction conditions: start temperature: 50 °C; iron content: 10 wt%; salt solvent: DI water; lignin solvent: DI water, methanol, acetone or tetrahydrofuran)

appearances of the prepared samples. Sample temperature vs reaction time is illustrated in Fig. 6. CO_2 and NO_2 concentration levels during preparation of Fe-lignin composites with different solvents are plotted in Fig. 7.

During preparation of Fe-lignin-W composite, Ts of Fe-lignin-water mixture started at 50 °C and increased gradually to 52.4 °C after adding iron nitrate solution to lignin-water suspension and mixing for 200 s. The temperature increase may result from the partial chelating of Fe^{3+} ions to the functional groups on the lignin surface. No gaseous CO_2, NO_2, or other volatile products formed (Fig. 7), meaning no Fe^{3+} reduction reaction or Fenton reaction occurred during the Fe-lignin-W co-precipitation process. Kraft lignin is completely insoluble in water at low temperature and most of the functional groups are unreachable to iron ions [3]; therefore, the reduction reaction of Fe^{3+} by active functional groups can be neglected in the precipitation process. Additionally, the Fenton reaction is not initialized since no peroxide species are present in the Fe-lignin-water suspension, thus, no CO_2 and NO_2 species are generated. A suspension mixture was formed during the stirring process with no solid deposition from the mixed solution. Most of the iron salt was deposited on the surface of lignin particles, and a brown powder product was noted as the Fe-lignin-W composite after evaporating water at room temperature (Fig. 8).

For the Fe-lignin-M precipitation process, the temperature increased from 50 °C to 57.9 °C after mixing for 110 s, then increased slowly to 58.9 °C after reaction for 200 s. Kraft lignin can be partially dissolved in methanol, thus, numerous functional groups are accessible and can combine with iron ions. Only a small amount of CO_2 was formed

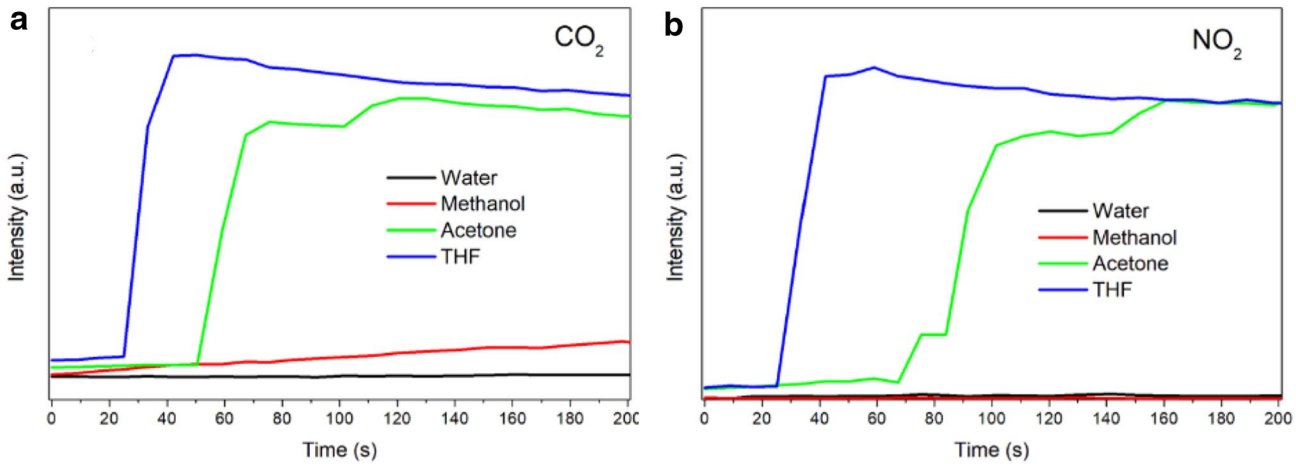

Fig. 7 CO_2, and NO_2 concentration levels by an on-line mass spectrometer during preparation of Fe-lignin composites with different solvents (reaction conditions: start temperature: 50 °C; iron content: 10 wt%; salt solvent: DI water; lignin solvent: DI water, methanol, acetone or tetrahydrofuran)

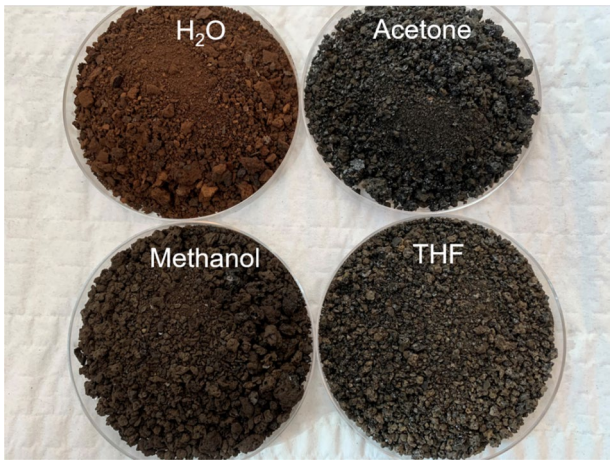

Fig. 8 Physical appearance of 10% Fe-lignin composites prepared with different solvents: THF, acetone, methanol and DI water

but no NO_2 was detected during the precipitation process. CO_2 and part of the generated heat resulted from the oxidation of active species by Fe^{3+} ions. However, due to lack of peroxide species in the solution, hydroxyl radicals were not created, Fenton reaction was not initialized, and lignin decomposition did not take place in the Fe-lignin-methanol mixture. A sticky slurry mixture was made after stirring the mixture for 30 min. A mixture of brown and grey powder was produced after vaporizing methanol and water at room temperature (Fig. 8).

When using acetone as the solvent to prepare the Fe-lignin composite, the temperature increased from 50 °C to 58 °C after mixing for 40 s, then increased gradually to 62.3 °C after reaction for 200 s (Fig. 6). Before the temperature reached 58 °C, the reaction was mild with only a trace of CO_2 generated. Then the reaction became severe, with large amounts of gases including CO_2, NO_2, and solvents (acetone and water vapor) bubbling out of the mixture (Fig. 7), while expanding to a foam state which dried to a porous structure. This means both the Fe^{3+} reduction reaction and Fenton reaction were triggered during the Fe-lignin-A co-precipitation process. Similar to THF, acetal peroxides may form when acetone is exposed to air [56, 57], leading to creation of hydroxyl radicals by peroxide species through Fenton reaction; consequently, redox reaction of lignin is triggered to produce CO_2 and NO_2. A dark grey powder product was produced as Fe-lignin-A composite (Fig. 8).

When mixing iron nitrate solution and lignin-THF solution at 50 °C, the Fenton reaction was fierce and the temperature increased rapidly from 50 °C to 63 °C in 22 s. The Fe-lignin mixture was puffed by CO_2, NO_2, and vaporized solvents, and quickly solidified and dried forming a porous black material. A dark grey powder product was made after drying the sample at room temperature for one week (Fig. 8).

FTIR spectra of Kraft lignin and Fe-lignin composites prepared with four different solvents are compared in Fig. 9. All the FTIR bands related to -OH (3368 cm^{-1} and 1078 cm^{-1}) -C = O, C–O–C, and -COO (1710, 1640, 1458, 1367, 1215, and 1078 cm^{-1}) are changed in intensity and/or shifted in position. The lessening of the intensity and shift of the peaks are contributed by the interaction between Fe ions and hydroxyl, carboxyl, carbonyl, ether and ester functional groups in Kraft lignin, i.e., Fe ions are chelated to -OH, -C = O, C–O–C, and -COO during the coprecipitation process [52]. The decrease in the intensity of -OH, C = O, and C-O related groups for Fe-lignin composites is ordered Fe-lignin-T > Fe-lignin-A > Fe-lignin-M > Fe-lignin-W. The intensity of FTIR bands (1535 and 1330 cm^{-1}) of surface nitrate complexes [53–55] increases with the order of Fe-lignin-W < Fe-lignin-M < Fe-lignin-A < Fe-lignin-T [3]. This implies that the dispersion rates of

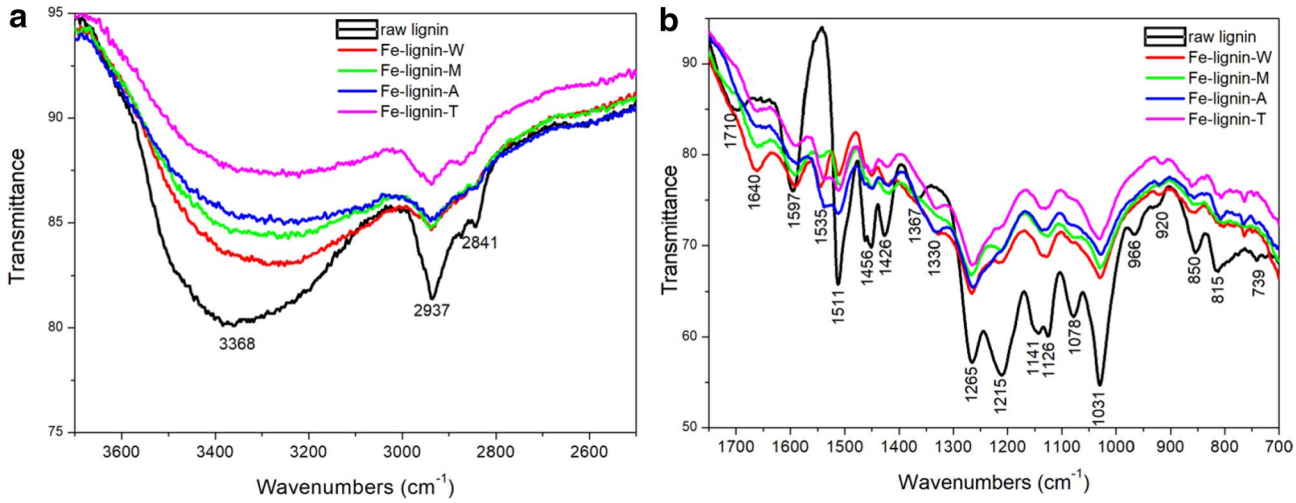

Fig. 9 FTIR spectra of Kraft lignin and Fe-lignin composites prepared with different solvents at the ranges of 3700 to 2500 cm^{-1} (**a**) and 1750 to 700 cm^{-1} (**b**)

Fe ions in Kraft lignin are increasing following an order of Fe-lignin-W < Fe-lignin-M < Fe-lignin-A < Fe-lignin-T. FTIR results indicate a better dispersion of iron ions in Kraft lignin will be achieved when Kraft lignin is completely dissolved by an organic solvent.

The SEM images (Fig. 10) show the morphologies of Fe-lignin composites prepared with four different solvents. The morphology of the Fe–lignin-W composite is much different from those of Fe-lignin-M, Fe-lignin-A, and Fe-lignin-T composites. Large iron particles observed on the surface of Fe-lignin-W composite are due to the poor solubility of Kraft lignin in water [3]; iron deposits and agglomerates on the lignin surface since kraft lignin is not dissolved, and presents as a condensed chunk. Diameter of the surface iron particles of Fe-lignin-W sample was about 20–200 nm (Fig. 10a). Iron particles are smaller in Fe-lignin-M composite, and their diameters range between 10–20 nm (Fig. 10b). For the Fe-lignin-A composite, fewer particles are observed on the surface (Fig. 10c) since iron ions are uniformly chelated by the functional groups in lignin. The morphology of Fe-lignin-T composite is homogeneous (Fig. 10d). Fe ions should be well distributed in the lignin matrix, therefore, no iron particles are observed to form on the surface of the composite. Spherical iron nanoparticles were uniformly distributed in the carbon matrix after thermal decomposition of Fe-lignin-T composites [3]. XRD results proved that these nanoparticles were composed of α-Fe, γ-Fe, iron carbide, and graphene structures [2, 3].

3.3 Fe-lignin Composites with Different iron Concentration

The effect of iron content on the formation of Fe-lignin composites through coprecipitation method was investigated. Iron-lignin composites with four different iron contents were prepared using THF for dissolution of Kraft lignin: 5 wt%, 10 wt%, 15 wt% and 20 wt%. 5% Fe-lignin, 10% Fe-lignin, 15% Fe-lignin, and 20% Fe-lignin exhibited different characteristics during the coprecipitation process, i.e., different start time of the Fenton reaction, temperature profiles, gas formation rate and amount, and physical appearances of the dried samples. Sample temperature vs reaction time is plotted in Fig. 11. CO_2 and NO_2 concentration levels during preparation of Fe-lignin composites with different solvents are plotted in Fig. 12.

Temperature profiles are distinct for the formation of Fe-lignin composites through coprecipitation process (Fig. 11). For the 5% Fe-lignin sample, its temperature increased gradually from 45 °C to 49.5 °C after adding iron solution to lignin solution for 20 s. Temperature of 10% Fe-lignin increased quickly from 45 °C to 55.5 °C in 20 s after blending both iron and lignin solutions, while the temperatures for 15% and 20% Fe-lignin samples increased abruptly 45 °C to 66.3 °C and 79.1 °C in 20 s, respectively. The maximum temperature for each sample is 54 °C after 200 s, 63 °C after 144 s, 69.7 °C after 50 s, and 79.7 °C after 32 s for 5%, 10%, 15% and 20% Fe-lignin samples, respectively. Fenton

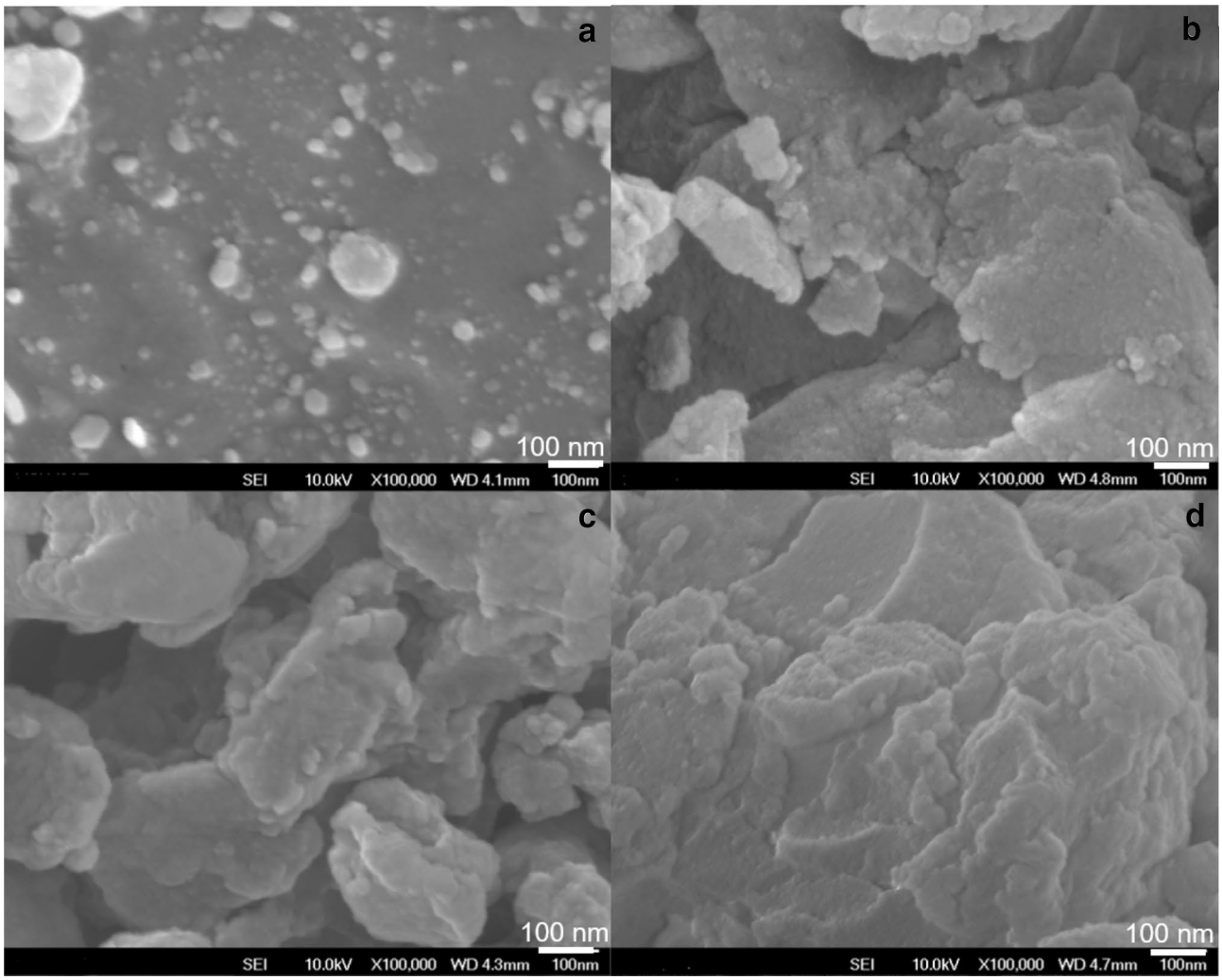

Fig. 10 SEM images of 10% Fe-lignin composites prepared with different solvents: **a** Fe-lignin-W, **b** Fe-lignin-M, **c** Fe-lignin-A, and **d** Fe-lignin-T

reaction induction time was shorter with increase of iron content (Fig. 12); the initiation times were 50 s, 25 s, 9 s, and 1 s for 5%, 10%, 15% and 20% Fe-lignin samples, respectively. High initial metal concentration in the solution and the abundant availability of the active functional groups on the Kraft lignin at the beginning of the process can kinetically accelerate the rate of the chelating and Fenton reactions [32]. With lower iron concentration, there is gradual chelation of the active sites resulting in less heat generation and less Fe^{3+} reduced to Fe^{2+}. As a result, there is a lower rate of Fenton reaction since it depends on Fe^{2+} level and solution temperature. With increase of Fe^{3+} concentration, more Fe^{2+} was generated, and more heat was liberated to the mixture. The Fenton reaction was then accelerated to create more hydroxyl radicals; consequently, the rate of oxidation of lignin was further promoted and more heat and gaseous products were produced.

FTIR spectra of Kraft lignin and Fe-lignin composites with different iron content are plotted in Fig. 13. The intensity of the peaks related to the free hydroxyl groups (3700–3300 cm^{-1} and 1100–900 cm^{-1}) in Kraft lignin attenuates with increasing of iron content, which is attributed to the decrease of the free hydroxyl groups on the Kraft lignin [3]. The intensity of the peak at 3220 cm^{-1}, which is the -OH stretching vibration of iron hydroxyl, increases with higher iron content because iron hydroxyl content increases with more iron content. The intensity of the peaks related to C = O, C–O–C and -COO groups also decreases with increase of iron content. Attenuated intensity of free hydroxyl, C = O, and C-O groups means more iron ions chelated to carbonyl, carboxyl, and hydroxyl groups with increasing iron content [3].

Figure 14 demonstrates physical appearance of Fe-lignin composites with different iron content. The color of

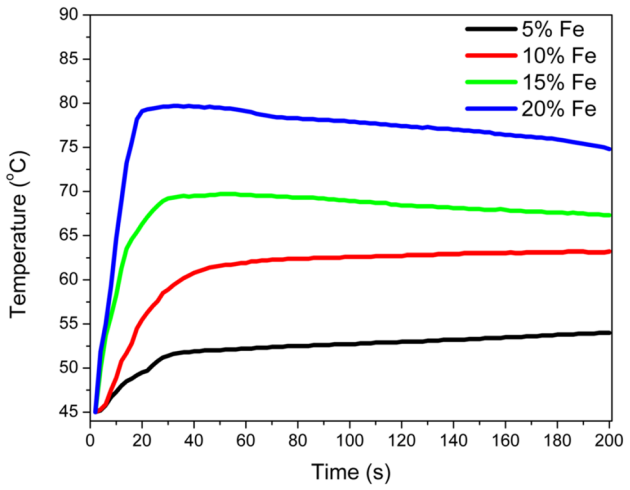

Fig. 11 Temperature profiles during preparation of Fe-lignin composites with different iron content (reaction conditions: start temperature, 45 °C; iron content, 5 wt%, 10 wt%, 15 wt% and 20 wt%; salt solvent, DI water; lignin solvent, tetrahydrofuran)

Fe-lignin composites changed from black (5%) to dark gray (10% and 15%) to light brown (20%). Increased iron content increased the amount of $Fe(OH)_3$ that was formed and distributed in the composite which could explain the color change. The Fe-lignin composite became finer with increase of iron content because more functional groups and other chemical bonds in lignin are oxidized or broken as more iron ions participate in the Fenton reaction. As a result, depolymerization degree of lignin is increased.

Figure 15. shows SEM images of Fe-lignin samples with 5%, 10%, 15% and 20% iron content. Nanoparticles were found embedded in lignin matrices and the numbers and sizes of particles increased with increase of iron content [58].

3.4 The Effect of the Initial Mixing Temperature

The Fenton reaction is an exothermic process and the reaction rate increases with increasing temperature, with the effect more obvious at low initial temperatures; therefore, temperature is one of the important factors influencing reaction kinetic rates in Fenton reaction. Monitoring the temperature and controlling the rise in temperature is critical to safely manage the reaction. Experiments were conducted at 45 °C, 50 °C, 55 °C and 60 °C to explore the effect of initial temperature on the chemical coprecipitation of 10% Fe-lignin composite. Figure 16 demonstrates temperature profiles during preparation of Fe-lignin composites with different start temperature. An increase in initial temperature leads to an accelerated initial kinetic rate of Fenton reaction and consequently, an increase in system temperature. The induction time of the Fenton reaction is shortened. When the coprecipitation started with an initial temperature of 60 °C, the reaction was so fierce, the Fenton reaction was triggered immediately. Tremendous amounts of gaseous products and vapors were released from the mixture as the temperature shot from 60 °C to 80.5 °C in 10 s and reached 90 °C in 30 s. Reactants were solidified as a foam state and puffed out of the glass beaker by the gases and vapors. If the initial temperature is 60 °C or above, thermal runaway can occur

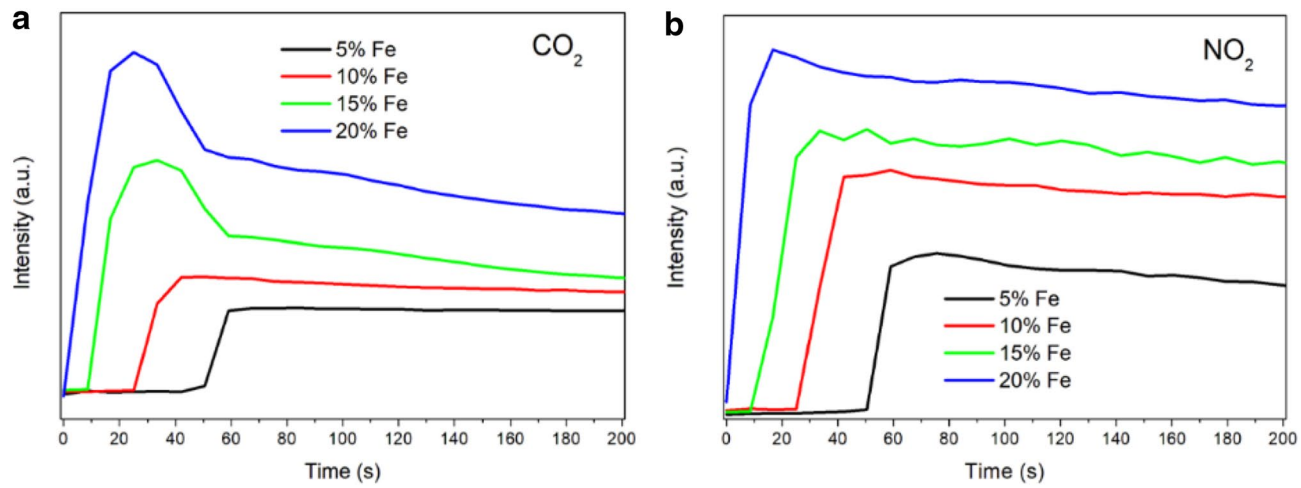

Fig. 12 CO_2 and NO_2 concentration levels by an on-line mass spectrometer during preparation of Fe-lignin composites with different iron content (reaction conditions: start temperature, 45 °C; iron, 5 wt%, 10 wt%, 15 wt% and 20 wt%; salt solvent, DI water; lignin solvent, tetrahydrofuran)

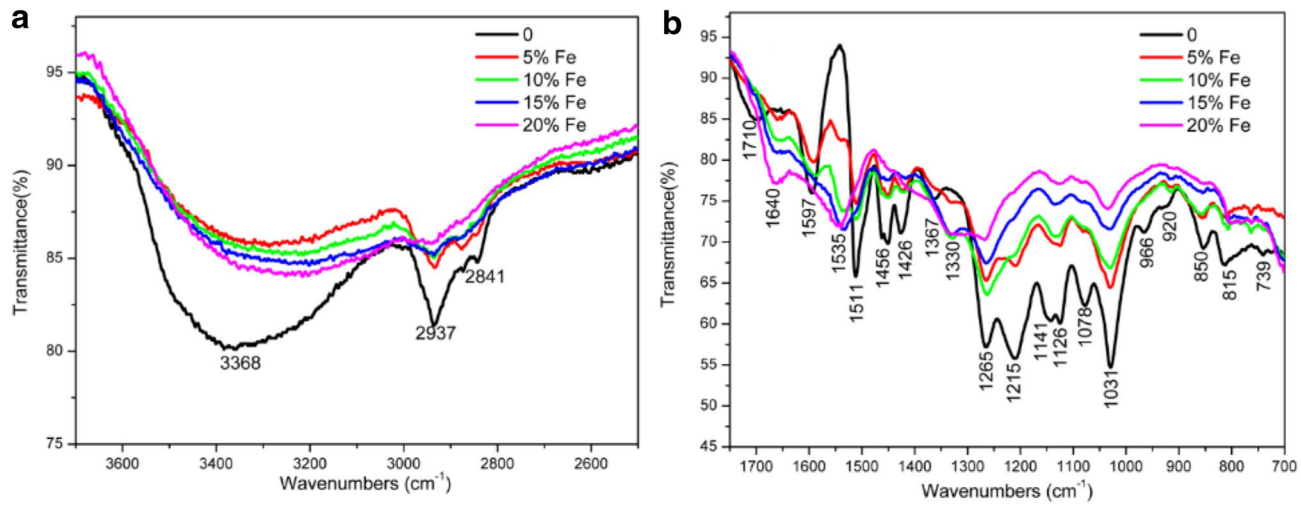

Fig. 13 FTIR spectra of raw KL, and Fe-lignin composites with different iron content at the ranges of 3700 to 2500 cm^{-1} (**a**) and 1750 to 700 cm^{-1} (**b**)

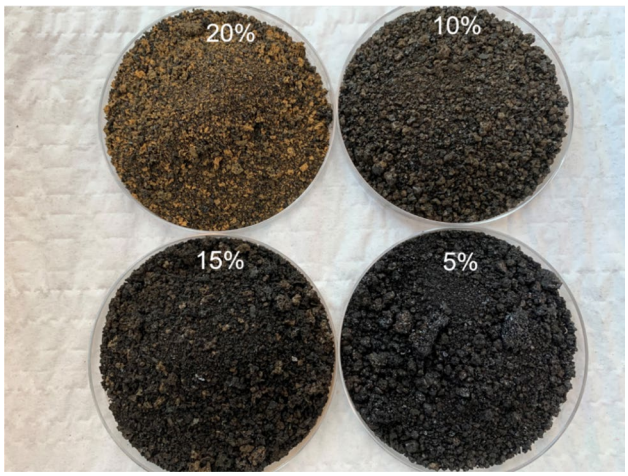

Fig. 14 Physical appearances of Fe-lignin composites with different iron content

occasionally due to the accelerated initial reaction rate, and subsequently, more heat from Fenton reaction accumulating in the system leading to rapid temperature increase where solvents are vaporized in a very short time (< 60 s). The active functional groups in lignin then undergo catalytic ignition by Fe^{3+} ions when exposed to air and the dried Fe-lignin powder starts to burn.

The effects of types of transition metals, solvents, concentration of metal salts, and initial solution temperature on the interactions between metal ions and Kraft lignin were investigated and the phenomenon observed during the preparation process are summarized in Table 3.

To prepare a M-lignin composite with the best miscibility, the following is the most reliable process developed: THF and acetone are appropriate solvents to dissipate Kraft lignin; to avoid the potential for thermal runaway, the coprecipitation process should be executed at room temperature if copper nitrate or iron nitrate are used as the metal salts; and metal loading should be 15% or less. The coprecipitation process should not be performed in a batch reactor. A continuous flow mixing method is suggested to prepare M-lignin in massive scale by chemical coprecipitation process.

4 Conclusions

The results of the current study have shown metal-lignin composites can be prepared though a coprecipitation method. However, it was observed the coprecipitation process was exothermic and significant heat and gases were released from oxidation of lignin by Fenton or Fenton-like reactions. The structure, uniformity, morphology, physical appearance, and metal particle size of the metal-lignin composites are greatly influenced by types of transition metals, solvents, initial temperature and concentration of metal salt.

Transition elements, namely Fe(III), Ni(II), Cu(II), and Mo(VI, $(Mo_7O_{24})^{6-}$) were examined to prepare metal-lignin composites by coprecipitation method. The reactions of coprecipitation with different metals behaved distinctively in process temperature, gaseous products, physical appearances, morphology, and structure of the solid products. No gaseous or volatile products formed during Mo-lignin

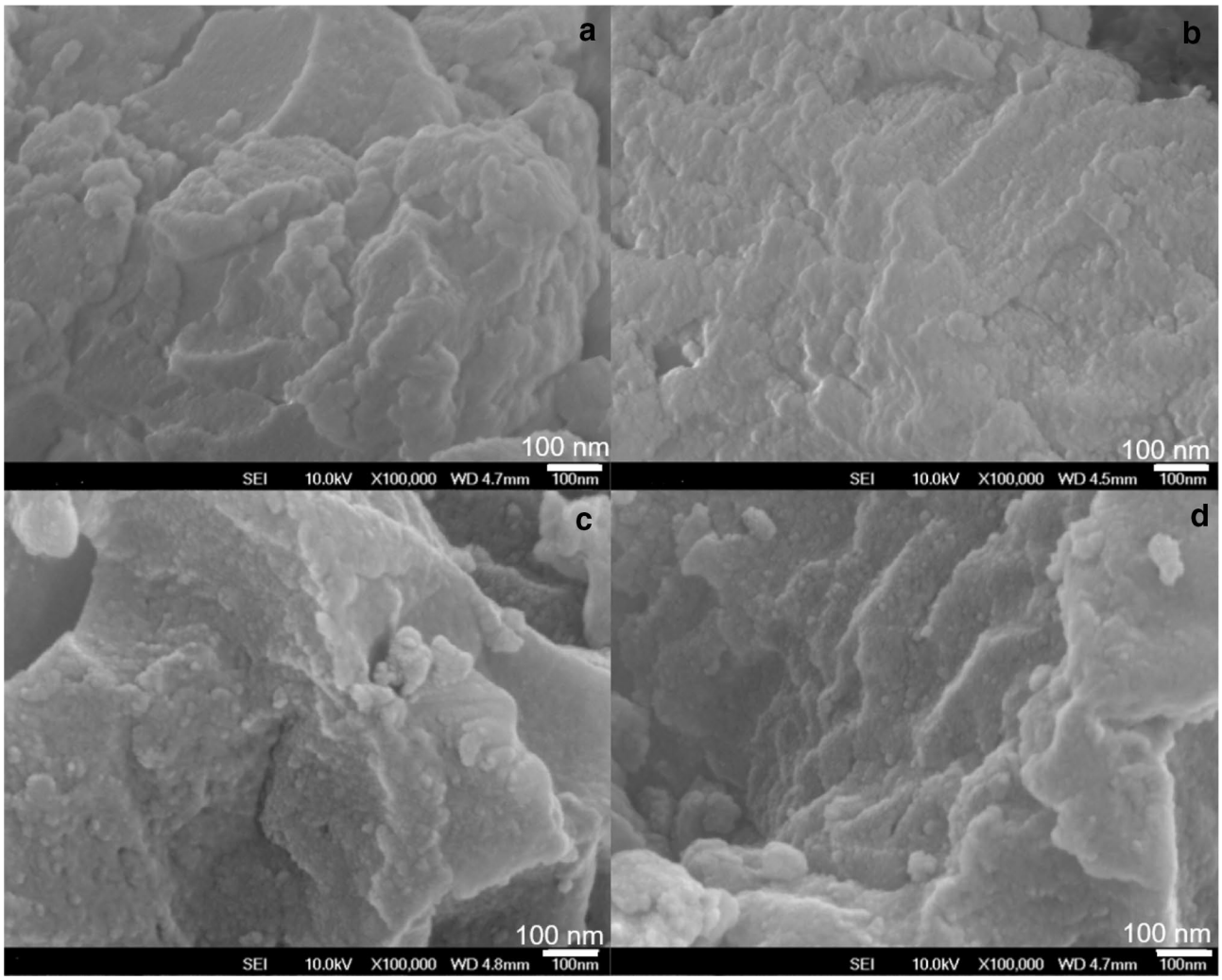

Fig. 15 SEM images of Fe-lignin composites with different iron content: **a** 5 wt%, **b** 10 wt%, **c** 15 wt% and **d** 20 wt%

co-precipitation process. No interaction or very weak interaction occurs between lignin and Mo(VI) ions when temperature is kept constant and no gaseous products are detected during the coprecipitation process. Ni ions are strongly chelated by oxygen-containing ligands in lignin, but no redox or Fenton-like reaction occurs during Ni-lignin coprecipitation process. Fe^{3+} and Cu^{2+} ions are combined to the functional groups and then quickly trigger the oxidation of lignin through Fenton or Fenton-like reaction. Significant heat and gaseous products (NO_2 and CO_2) are formed in the precipitation procedure.

DI water, methanol, acetone, and THF were investigated to dissolve Kraft lignin for the Fe-lignin coprecipitation. The Fenton reaction will not happen when using water or methanol but will occur when tetrahydrofuran or acetone are used to dissolve Kraft lignin. Peroxides may be formed in THF and acetone if exposed to air, triggering the Fenton reaction with the existence of Fe or Cu ions. The intensity

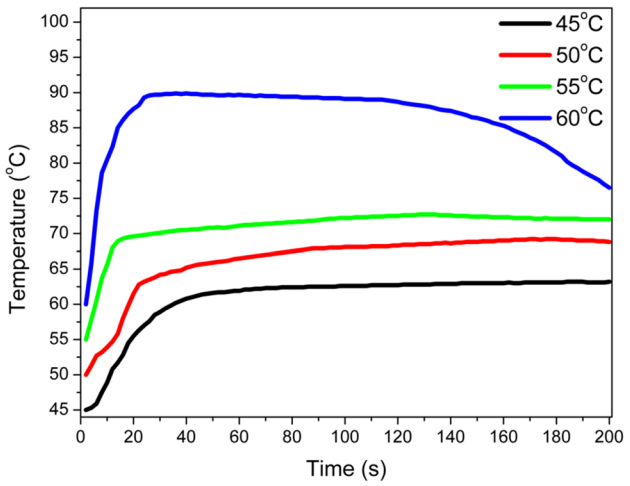

Fig. 16 Temperature profiles during preparation of Fe-lignin composites with different start temperature (reaction conditions: start temperature: 45 °C, 50 °C, 55 °C and 60 °C; iron content, 10 wt%; salt solvent, DI water; lignin solvent, tetrahydrofuran)

of reaction is in the order of Fe-lignin-T > Fe-lignin-A > Fe-lignin-M > Fe-lignin-W; the degree of iron dispersion is in the same order. The effect of iron content on the formation of Fe-lignin composite is studied, and it is found the reaction initialization time is shortened and the reaction becomes more vigorous and uncontrollable with increase of iron content. Temperature is one of the important factors influencing kinetic rates in Fenton reaction. The coprecipitation process becomes less controllable with increase of initial mixing temperature, and it is discovered that thermal runaway reaction might happen if the mixing start temperature reached 60 °C or above.

Table 3 Conditions and observations for M-lignin preparation by the coprecipitation method

M-lignin composites	Solvent for lignin dissolution	Initial coprecipitation temperature (°C)	Fenton/Fenton-like reactions?	Exothermic process?	Potential thermal runaway?	Miscibility
20% Mo-lignin	THF	45	No	No	No	Good[a]
10%Ni-lignin	THF	45	No	Yes, medium	No	Good[a]
10% Cu-lignin	THF	45	Yes	Yes, strong	Yes	Excellent[a]
10% Fe-lignin	THF	45	Yes	Yes, strong	Yes	Excellent[a]
10% Fe-lignin	DI water	50	No	Yes, weak	No	Poor[b]
10% Fe-lignin	Methanol	50	No	Yes, medium	No	Fair[b]
10% Fe-lignin	Acetone	50	Yes	Yes, strong	Yes	Excellent[b]
10% Fe-lignin	THF	50	Yes	Yes, strong	Yes	Excellent[b]
5% Fe-lignin	THF	45	Yes	Yes, medium	Maybe in large scale	Excellent[c]
15% Fe-lignin	THF	45	Yes	Yes, very strong	Yes	Good[c]
20% Fe-lignin	THF	45	Yes	Yes, extreme	Yes	Fair, iron agglomeration
10% Fe-lignin	THF	55	Yes	Yes, extreme	Yes	Excellent
10% Fe-lignin	THF	60	Yes	Yes, extreme	Yes, even at lab-scale	–

[a]Agrees with results of reference [30]

[b]Agrees with results of reference [3]

[c]Agrees with results of reference [58]

Acknowledgements This work was supported by the USDA Forest Service through Grant Nos. 19-JV-11111124-053 and 19-JV-11111124-063. The authors would like to acknowledge Domtar Corp., North Carolina for providing Kraft lignin for this study. Neil Gribbins and Timothy Ketelboeter at USDA Forest Products Laboratory provided editorial assistance.

References

1. F.J. Maldonado-Hódar, C. Moreno-Castilla, J. Rivera-Utrilla, Y. Hanzawa, Y. Yamada, Catalytic Graphitization of Carbon Aerogels by Transition Metals. Langmuir **16**, 4367–4373 (2000)
2. Q. Yan, J. Li, X. Zhang, C. Wang, J. Zhang, Z. Cai, Mass Production of Graphene Materials from Solid Carbon Sources using A Molecular Cracking and Welding Method. J. Mater. Chem. A. **7**, 13978–13985 (2019)
3. Q. Yan, Z. Cai, Effect of Solvents on Fe–Lignin Precursors for Production Graphene-Based Nanostructures. Molecules **25**, 2167 (2020)
4. Q. Yan, J. Li, X. Zhang, J. Zhang, Z. Cai, Synthetic Bio-Graphene Based Nanomaterials through Different Iron Catalysts. Nanomaterials **8**, 840 (2018)
5. V. Torrisi, F. Ruffino, Metal-Polymer Nanocomposites: (Co-) Evaporation/(Co)Sputtering Approaches and Electrical Properties. Coatings **5**, 378–424 (2015)
6. F. Faupel, V. Zaporojtchenko, T. Strunskus, H. Greve, U. Schürmann, H. Takele, R. Podschun, Functional Polymer Nanocomposites. Polym. Polym. Compos. **16**, 471–481 (2008)
7. H. Biederman, L. Martinu, D. Slavinska, I. Chudacek, Plasma deposition and properties of composite metal/polymer and metal/hard carbon films. Pure Appl. Chem. **60**, 607–618 (1988)
8. L. Balan, D. Burget, Synthesis of metal/polymer nanocomposite by UV-radiation curing. Eur. Polymer J. **42**, 3180–3189 (2006)
9. Th Peter, S. Rehders, U. Schürmann, T. Strunskus, V. Zaporojtchenko, F. Faupel, High rate deposition system for metal-cluster/SiOxCyHz–polymer nanocomposite thin films. J. Nanopart. Res. **15**, 1710 (2013)
10. N.A. Zulina, I.M. Pavlovetc, M.A. Baranov, I.Y. Denisyuk, Optical, structural and nonlinear optical properties of laser ablation synthesized Ag nanoparticles and photopolymer nanocomposites based on them. Opt. Laser Technol. **89**, 41–45 (2017)
11. Ehsani, A., Bigdeloo, M., Ansari, M. Y., Mirtamizdoust, B., Heidari, A. A., Hadi, M., Shiri, H. M. Nanocomposite of Conjugated Polymer/Nano-Flowers Cu(II) Metal-Organic System with 2-Methylpyridinecarboxaldehyde Isonicotinohydrazide as a Novel and Hybrid Electrode Material for Highly Capacitive Pseudocapacitors. Bull. Chem. Soc. Jpn. 91, 617- (2018).
12. S.K. Krishnan, E. Singh, P. Singh, M. Meyyappan, H.S. Nalwa A review on graphene-based nanocomposites for electrochemical and fluorescent biosensors. RSC Adv. 9, 8778–8881 (2019).
13. G. Maggioni, A. Vomiero, S. Carturan, C. Scian, G. Mattei et al., Structure and optical properties of Au-polyimide nanocomposite films prepared by ion implantation. Appl. Phys. Lett. **85**, 5712 (2004)
14. F.F. Shi, Recent advances in polymer thin films prepared by plasma polymerization Synthesis, structural characterization, properties and applications. Surf. and Coatings Technol. **82**, 1–15 (1996)
15. V. Shanmugavalli, K. Vishista, An Investigation on the Supercapacitive Performance of CuCo2O4/Polyaniline, a Nanocomposite of Spinel Structured Transition Binary Metal Oxide and Conducting Polymer, with a Special Focus on Bonding and Electron Density Distribution Through MEM. J Inorg Organomet Polym **30**, 1448–1462 (2020)
16. S.H. Lee, B.-H. Jun, Silver Nanoparticles: Synthesis and Application for Nanomedicine. Int. J. Mol. Sci. **20**, 865 (2019)
17. P. Biehl, M. Von der Lühe, S. Dutz, F.H. Schacher, Synthesis, Characterization, and Applications of Magnetic Nanoparticles Featuring Polyzwitterionic Coatings. Polymers **10**, 91 (2018)
18. S.W. Lee, J.K. Kumpfer, P.A. Lin, G. Li, X.P.A. Gao, S.J. Rowan, R.M. Sankaran, In Situ Formation of Metal Nanoparticle Composites via "Soft" Plasma Electrochemical Reduction of Metallosupramolecular Polymer Films. Macromolecules **45**, 8201–8210 (2012)
19. G. Nesher, G. Marom, D. Avnir, Metal−Polymer Composites: Synthesis and Characterization of Polyaniline and Other Polymer@Silver Compositions. Chem. Mater. **20**, 4425–4432 (2008)
20. G.I. Dzhardimalieva, I.E. Uflyand, Design Strategies of Metal Complexes Based on Chelating Polymer Ligands and Their Application in Nanomaterials Science. J Inorg Organomet Polym **28**, 1305–1393 (2018)
21. P.S. Thue, E.C. Lima, J.M. Sieliechi, C. Saucier, S.L.P. Dias, J.C.P. Vaghetti, F.S. Rodembusch, F.A. Pavan, Effects of first-row transition metals and impregnation ratios on the physicochemical properties of microwave-assisted activated carbons from wood biomass. J Colloid. Interface Sci. **486**, 163–175 (2017)
22. Y. Wang, B. Yu, K. Liu, X. Yang, M. Liu, T.-S. Chan, X. Qiu, J. Li, W. Li, Co single-atoms on ultrathin N-doped porous carbon by biomass complexation strategy for high performance metal-air batteries. J. Mater. Chem. A. **8**, 2131–2139 (2020)
23. G. Sharma, D. Kumar, A. Kumar, A.H. Al-Muhtaseb, D. Pathania, M. Naushad, G.T. Mola, Revolution from monometallic to trimetallic nanoparticle composites, various synthesis methods and their applications: A review. Mater Sci Eng C Mater Biol Appl. **71**, 1216–1230 (2017)
24. Rane, A. V., Kanny, K., Abitha, V.K., S. Thomas, in Synthesis of Inorganic Nanomaterials: Advances and Key Technologies, Sneha Mohan Bhagyaraj, Oluwatobi Samuel Oluwafemi, Nandakumar Kalarikkal, Sabu Thomas (Eds.), Woodhead Publishing, pp. 121–139 (2018).
25. A. Ali, H. Zafar, M. Zia, I. Haq, A.R. Phull, J.S. Ali, A. Hussain, Synthesis, characterization, applications, and challenges of iron oxide nanoparticles. Nanotechnol. Sci. Appl. **9**, 49–67 (2016)
26. ASTM D4442–07(2007). Standard Test Methods for Direct Moisture Content Measurement of Wood and Wood-Based Materials, ASTM Int.: West Conshohocken, PA, USA, 2007.
27. ASTM D1102–84(2007). Standard Test Method for Ash in Wood, ASTM Int.: West Conshohocken, PA, USA, 2007.
28. T.K. Nguyen, N. Thanh, S. Maclean, Mahiddine, Mechanisms of Nucleation and Growth of Nanoparticles in Solution. Chem. Rev. **114**, 7610–7630 (2014)
29. B. Wang, Y. Sun, R. Sun, Fractionational and structural characterization of lignin and its modification as biosorbents for efficient removal of chromium from wastewater: a review. J. Leather Sci. Eng. **1**, 5 (2019)
30. Q. Yan, J. Li, X. Zhang, C. Wang, J. Zhang, Z. Cai, Catalytic Graphitization of Kraft Lignin to Graphene-based Structures with Four Different Transition Metals. J. Nanopart. Res. **20**, 223 (2018)
31. R. Garcia-Valls, T.A. Hatton, Metal ion complexation with lignin derivatives. Chem. Eng. J. **94**, 99–105 (2003)
32. J. Ma, K. Zhang, M. Huang, S.B. Hector, B. Liu, C. Tong, Q. Liu, J. Zeng, Y. Gao, T. Xu, Y. Liu, X. Liu, Y. Zhu, Involvement of Fenton chemistry in rice straw degradation by the lignocellulolytic bacterium Pantoeaananatis Sd-1. Biotechnol Biofuels **9**, 211 (2016)
33. H.Y. Chen, Why the Reactive Oxygen Species of the Fenton Reaction Switches from Oxoiron(IV) Species to Hydroxyl

Radical in Phosphate Buffer Solutions? A Computational Rationale. ACS Omega **4**, 14105–14113 (2019)
34. R.F.N. Quadrado, A.R. Fajardo, Fast decolorization of azo methyl orange via heterogeneous Fenton and Fenton-like reactions using alginate-Fe^{2+}/Fe^{3+} films as catalysts. Carbohydr Polym. **177**, 443–450 (2017)
35. Q. Yan, C.R. Boardman, Z. Cai, Thermal stability of metal-lignin composites prepared by coprecipitation method. Thermochim. Acta **690**, 178659 (2020)
36. T.K. Kirk, M.D. Mozuch, M. Tien, Free hydroxyl radical is not involved in an important reaction of lignin degradation by Phanerochaete chrysosporium Burds. Biochem. J. **226**, 455–460 (1985)
37. Pagano, M., Volpe, A., Lopez, A. MascoloG. & Ciannarella R. Degradation of chlorobenzene by Fenton-like processes using zero-valent iron in the presence of Fe^{3+} and Cu2+, Environmental Technology. 32, 155–165(2011).
38. N.K. Urbański, A. Beresewicz, Generation of *OH initiated by interaction of Fe^{2+} and Cu^{+} with dioxygen, comparison with the Fenton chemistry. Acta Biochim Pol. **47**, 951–962 (2000)
39. T. Arakaki, C. Anastasio, Y. Kuroki, H. Nakajima, K. Okada, Y. Kotani, D. Handa, S. Azechi, T. Kimura, A. Tsuhako, Y. Miyagi, A General Scavenging Rate Constant for Reaction of Hydroxyl Radical with Organic Carbon in Atmospheric Waters. Environ. Sci. Technol. **47**, 8196–8203 (2013)
40. M.C. Pereira, L.C.A. Oliveira, E. Murad, Iron oxide catalysts: Fenton and Fenton-like reactions - a review. Clay Miner. **47**, 285–302 (2012)
41. S. Garcia-Segura, J.D. Ocon, M.N. Chong, Electrochemical Oxidation Remediation of Real Wastewater Effluents – A review. Process Saf. Environ. Prot. **113**, 48–67 (2018)
42. S. Garcia-Segura, E. Brillas, L. Cornejo-Ponce, R. Salazar, Effect of the Fe^{3+}/Cu^{2+} ratio on the removal of the recalcitrant oxalic and oxamic acids by electro-Fenton and solar photoelectro-Fenton. Sol. Energy **124**, 242–253 (2015)
43. L. Zhang, Y. Xing, C. Liu, X. Zhou, H. Shi, Label-free colorimetric detection of Cu2+ on the basis of Fenton reaction-assisted signal amplification with unmodified gold nanoparticles as indicator. Sensors and Actuators B Chemical **215**, 561–567 (2015)
44. Stark, N.M., Yell, D.J., Agarwal, U.P. Techniques for characterizing lignin, O. Faruk, M. Sain (Eds.), Lignin in Polymer Composites, William Andrew Applied Science Publishers, Kidlington, UK (2016).
45. Q. Yan, J. Li, J. Zhang, Z. Cai, Thermal Decomposition of Kraft Lignin under Gas Atmospheres of Argon. Hydrogen, and Carbon Dioxide, Polymers **10**, 729 (2018)
46. J. Chen, C. Liu, S. Wu, J. Liang, M. Lei, Enhancing the quality of bio-oil from catalytic pyrolysis of Kraft black liquor lignin. RSC Adv. **6**, 107970–107976 (2016)
47. K. Minu, K.K. Jiby, V.V.N. Kishore, Isolation and purification of lignin and silica from the black liquor generated during the production of bioethanol from rice straw. Biomass Bioenerg. **39**, 210–217 (2012)
48. H. Yang, Y. Xie, X. Zheng, Y. Pu, F. Huang, X. Meng et al., Comparative study of lignin characteristics from wheat straw obtained by soda-AQ and Kraft pretreatment and effect on the following enzymatic hydrolysis process. Bioresour. Technol. **207**, 361–369 (2016)
49. Szilágyi, I.M., Madarász, J., Hang,e .F, Pokol, G. Partial thermal reduction of ammonium paratungstate tetrahydrate. Partial thermal reduction of ammonium paratungstate tetrahydrate' J Therm Anal Calorim. 88,139–144 (2007).
50. S. Alizadeh, S.A. Hassanzadeh-Tabrizi, MoO_3 fibers and belts: molten salt synthesis, characterization and optical properties. Ceram Int. **41**, 10839–10843 (2015)
51. H.L. Wang, J.Y. Cui, W.F. Jiang, Synthesis, characterization and flocculation activity of novel Fe(OH)3-polyacrylamide hybrid polymer. Mater. Chem. Phys. **130**, 993–999 (2011)
52. R. Ashkenazy, L. Gottlieb, S. Yannai, Characterization of acetone-washed yeast biomass functional groups involved in lead biosorption. Biotechnol. Bioeng. **55**, 1–10 (1997)
53. J. Zawadzki, IR spectroscopic investigations of the mechanism of oxidation of carbonaceous films with HNO_3 solution. Carbon **18**, 281–285 (1980)
54. A.A. El-Hendawy, Influence of HNO3 oxidation on the structure and adsorptive properties of corncob-based activated carbon. Carbon **41**, 713–722 (2003)
55. I. Bautista-Toledo, J. Rivera-Utrilla, M.A. Ferro-Garcia, C. Moreno-Castilla, Influence of the oxygen surface complexes of activated carbons on the adsorption of chromium ions from aqueous solutions: Effect of sodium chloride and humic acid. Carbon **32**, 93–100 (1994)
56. R.J. Kelly, Review of Safety Guidelines for Peroxidizable Organic Compounds. Chem. Health Saf. **3**, 28–36 (1996)
57. D.E. Clark, Peroxides and Peroxide - Forming Compounds. Chem. Health Saf. **8**(5), 12–21 (2001)
58. Q. Yan, J. Li, X. Zhang, J. Zhang, Z. Cai, In situ formation of graphene-encapsulated iron nanoparticles in carbon frames through catalytic graphitization of Kraft lignin. Nanomater. Nanotechnol. **8**, 184798041881895 (2018)